



Sub-micrometer chemical imaging of dental adhesive/dentin interfaces via mid-infrared photothermal microscopy

Ryo Kato^{a,b,c,d} , Tomiki Iuchi^d, Yumika Ida^d, Kazuhide Yonekura^d, Kentaro Takeichi^a, Shogo Kawashima^c, Takeo Minamikawa^c, Takuo Tanaka^{a,b}, Taka-aki Yano^{a,b,*}, Keiichi Hosaka^{a,d,e,**}

^a Institute of Post-LED Photonics, Tokushima University, 2-1 Minamijosanjima-cho, Tokushima, Tokushima, 770-0856, Japan

^b Innovative Photon Manipulation Research Team, RIKEN Center for Advanced Photonics, Wako, Saitama, 351-0198, Japan

^c Department of Systems Innovation, Graduate School of Engineering Science, Osaka University, Osaka, 560-8531, Japan

^d Department of Conservative Dentistry, Tokushima University Graduate School of Biomedical Sciences, 3-18-15 Kuramotocho, Tokushima, Tokushima, 770-8504, Japan

^e Smart Innovations for Preventive and Restorative Dentistry Research Group, Department of Operative Dentistry, Faculty of Dentistry, Chulalongkorn University, 34 Henri-Dunant Rd, WangMai, PathumWan, Bangkok, 10330, Thailand

ARTICLE INFO

Keywords:

Mid-infrared photothermal microscopy
IR spectroscopy
Biomaterials
Dental adhesives

ABSTRACT

Dental adhesive bonding plays a critical role in restorative dentistry and ensures durable restoration. Despite advancements, bond failure remains a challenge due to polymerization heterogeneity at the adhesive-dentin interface, which is influenced by various factors such as micro-voids. Conventional analytical methods used for dental materials, such as micro-Raman and FTIR spectroscopy, have limitations, such as the interference of autofluorescence and lack of spatial resolution. This study employed mid-infrared photothermal (MIP) microscopy to visualize the molecular distribution and polymerization degree of dental adhesives at the sub-micrometer scale. MIP imaging enables high-resolution chemical mapping without interfering with autofluorescence. The present results revealed heterogeneous polymerization across the adhesive-dentin interface, with lower degree of conversion (DC) rates near the dentin owing to the presence of hybrid layers. Additionally, localized reductions in the DC rate were observed, likely caused by micro-voids that hindered polymerization due to oxygen-inhibited layers. These findings provide direct evidence of molecular heterogeneity in dental adhesives that was previously unattainable using conventional techniques. MIP microscopy offers enhanced spatial resolution and chemical specificity, making it a promising tool for studying biomaterial interfaces and improving adhesive formulations for reliable dental treatments.

1. Introduction

Dental adhesive bonding plays a crucial role in modern restorative dentistry by enabling minimally invasive treatments and improving the longevity of restorations [1,2]. Various dental adhesive systems have been developed to achieve durable bonding between restorative materials and dental hard tissues, particularly dentin [3,4]. These systems can be broadly classified into etch-and-rinse and self-etch adhesives [5, 6]. While bonding to enamel is relatively predictable because of its high mineral content and stable structure, dentin bonding remains more

challenging because of its complex composition, higher organic content, and continuous fluid movement [7,8]. Among the available strategies, the self-etch approach is widely regarded as the gold standard for dentin bonding because it simplifies the bonding procedure and reduces the risk of over-etching or incomplete resin infiltration [5,9]. Among self-etch adhesives, the two-step self-etch system demonstrated superior bonding reliability compared to one-step self-etch adhesives [10,11]. However, despite advancements in adhesive technology, bond failure remains a persistent issue, leading to complications, such as micro-leakage, secondary caries, and reduced restoration longevity [12,13].

This article is part of a special issue entitled: Advances in Chemical Imaging published in Optics Communications.

* Corresponding author. Institute of Post-LED Photonics, Tokushima University, 2-1 Minamijosanjima-cho, Tokushima, Tokushima 770-0856, Japan.

** Corresponding author. Institute of Post-LED Photonics, Tokushima University, 2-1 Minamijosanjima-cho, Tokushima, Tokushima, 770-0856, Japan.

E-mail addresses: yano.takaaki@tokushima-u.ac.jp (T.-a. Yano), hosaka@tokushima-u.ac.jp (K. Hosaka).

<https://doi.org/10.1016/j.optcom.2025.132108>

Received 5 March 2025; Received in revised form 10 June 2025; Accepted 10 June 2025

Available online 10 June 2025

0030-4018/© 2025 The Authors. Published by Elsevier B.V. This is an open access article under the CC BY license (<http://creativecommons.org/licenses/by/4.0/>).

The spatial heterogeneity of the resin–dentin interface is a key factor influencing the performance of dental adhesives. The polymerization degree of dental adhesives may vary within the interface owing to differences in oxygen inhibition, resin infiltration, and adhesive composition [14–16]. Furthermore, the physical properties of the adhesive layer, such as hardness, modulus, and mechanical stability, may not be uniform across the interface [17,18]. The presence of micro-voids, such as air bubbles entrapped during the bonding process, can further lead to localized weaknesses and compromise bonding durability [19]. However, direct evidence of such molecular-scale heterogeneity and its impact on adhesive performance has been limited, primarily owing to the lack of suitable analytical techniques capable of resolving the interface at sub-micrometer resolution [19]. So far, a few techniques have been exploited to analyze the polymerization behavior of adhesive layers at the interface between adhesive layers and dentin, such as destructive testing, while destructive testing does not allow the chemical characterization of the adhesive layer–dentin interfaces. Raman spectroscopy is a powerful chemical analytical technique that allows probing of chemical compositions in biological samples, such as tissues [20]. Chemical analysis of teeth using Raman spectroscopy has been reported in various contexts, including studies on caries [21], periodontal disease [22], and demineralization [23]. In Raman spectroscopic analysis of dental adhesives/dentin interfaces, one needs to employ relatively longer excitation wavelengths (785 or 1065 nm) to excite Raman scattering of adhesive layers and dentin; otherwise, the strong autofluorescence signal from the sample overwhelms the relatively weak Raman signal [24,25]. This deteriorates the spatial resolution of Raman imaging derived from the diffraction limit of light and the detection sensitivity of Raman scattering owing to the low scattering efficiency in the near-infrared region. The low detection sensitivity of the Raman scattering signal of dental materials limits the field of view for Raman imaging, which prevents investigation of the molecular distribution and the polymerization rate in adhesives/dentin interfaces. Another chemical imaging technique, FTIR spectroscopy, is an autofluorescence-free analytical technique that employs mid-IR light, which has low photon energies and does not excite the fluorescence of the molecules. Hence, it has been extensively used for the chemical characterization of adhesive layers and dentin. However, the spatial resolution of FTIR spectroscopy is limited to several micrometers or more because of the diffraction limit of mid-IR light, which is not sufficiently high to resolve heterogeneities in chemical compositions and their properties. Although AFM-based chemical imaging techniques, such as tip-enhanced Raman spectroscopy and Nano-IR, realize super-resolution chemical imaging [26–29], these techniques have field-of-view limitations, typically on the order of a few to 10 μm and the imaging configuration, where mechanical contact between a metallic tip and sample is required.

Herein, we employ an all-optical super-resolution mid-IR imaging technique called mid-infrared photothermal (MIP) microscopy to chemically visualize the interfacial molecular components and polymerization rate with around 500 nm spatial resolution. MIP microscopy is an emerging IR imaging technique that leverages both continuous visible and pulsed mid-IR beams to overcome the spatial resolution limitations of conventional IR imaging. Pulsed mid-IR light excites transient IR absorption, which can generate local sample heating and expansion, known as the photothermal effect. The photothermal responses of the sample modulate the optical responses of visible scattering or reflection light, according to Mie theory. Hence, the IR absorption of a sample can be measured by detecting the modulated optical responses of the visible probe light. One of the advantages of MIP microscopy is its sub-micrometer spatial resolution, which is determined by the wavelength of the continuous visible beam. Thus, MIP microscopy achieves both sub-micrometer spatial resolution beyond the diffraction limit of mid-IR light and high chemical specificity based on IR absorption [30–34]. Owing to its super-resolution chemical imaging capability, MIP microscopy has been applied in various fields such as biological cells and tissues [35,36], biomaterials, and polymers [37,38].

It has recently been employed to analyze the degree of curing in composite resins used for dental treatment and revealed the variation in curing degree with different filler concentrations [39,40].

In this study, we used MIP microscopy to determine the spatial distribution of the chemical compositions of dentin and adhesive layers, and the polymerization rate of adhesive layers at interfaces between the adhesive layers and dentin in human dentin. The spatial distribution of uncured monomers, polymers, and fillers in the adhesive layers was visualized with a spatial resolution of approximately 500 nm, without interference from autofluorescence. The heterogeneous distribution of the polymerization rate of adhesives at the sub-micrometer scale was also observed by examining the infrared vibrational modes of monomers and polymers in the adhesives. The optical images of the interfacial adhesive layers and chemical characterization results using MIP microscopy suggested that one of the causes for the local decrease in the polymerization rate in the adhesive layers was the generation of nano/microscale bubbles in the adhesive layers. The present results confirm the potential of MIP microscopy for the chemical characterization of not only interfaces between dentin and adhesive layers, but also other biocompatible materials used for biomedical applications, which opens new avenues for tooth science.

2. Results and discussion

We investigated slices of the extracted human teeth. Fig. 1(a) and (b) show a photograph of the sliced human tooth sample and an optical image of the cross-section of the mirror-polished human dentins exhibiting the composite resin (CR)/dental adhesive/dentin interface. It should be clarified that the samples were exposed to curing light prior to slicing. The light was irradiated from the top side (resin side) toward the bottom side (dentin side). After this visible light exposure, the tooth samples were sliced. The chemical structures of dominant monomer components of the adhesives were shown in Fig. 1(c). It should be noted that the content of Bis-GMA is around 40 % in our adhesives. Although the adhesives contain two monomers and the detailed polymerized structures have not yet been fully elucidated so far, previous studies revealed that the methacrylic bonds in both monomers are consumed during polymerization [24,25]. In Fig. 1(c), we have highlighted the methacrylic groups in the two monomers with red circles in order to facilitate estimation of the chemical structural changes in the adhesives before and after visible light irradiation. The IR vibrational modes of the dental adhesives and their evolution upon visible light irradiation were characterized using FTIR spectroscopy, as shown in Fig. 1(d). In the IR spectra, the primary IR absorption peak at 1454 cm^{-1} indicates the CH_2 bending mode of all organic compounds in the adhesives, the peaks at 1512 cm^{-1} and 1609 cm^{-1} indicate aromatic $\text{C}=\text{C}$ bonds in aromatic monomers and polymers, the peak at 1635 cm^{-1} indicates the aliphatic $\text{C}=\text{C}$ bonds in monomers, and the peak at 1716 cm^{-1} indicates $\text{C}=\text{O}$ bonds in all organic compounds. Exposure of dental adhesives to visible light results in the polymerization of monomers in dental adhesives, where aliphatic $\text{C}=\text{C}$ bonds are transformed into $\text{C}-\text{C}$ bonds. This was monitored by the change in the intensity ratio between the aliphatic $\text{C}=\text{C}$ bonds and aromatic $\text{C}=\text{C}$ bonds. In Fig. 1(d), the IR transmittance of the peaks at 1512 cm^{-1} and 1716 cm^{-1} did not show a significant change, while the peaks at 1635 cm^{-1} showed a gradual increase, indicating a decrease in aliphatic $\text{C}=\text{C}$ bonds in the monomers due to the conversion. The degree of conversion (DC) rate of the dental adhesives was evaluated in accordance with previous studies [24,25].

$$DC (\%) = \left\{ 1 - \frac{(I_{1635\text{ cm}^{-1}}/I_{1512\text{ cm}^{-1}})_{\text{after curing}}}{(I_{1635\text{ cm}^{-1}}/I_{1512\text{ cm}^{-1}})_{\text{before curing}}} \right\} \times 100$$

The distribution of chemical compositions at the dentin/adhesive interfaces was visualized using large-area high-resolution hyperspectral MIP imaging. The preparation way of our teeth sample was shown in

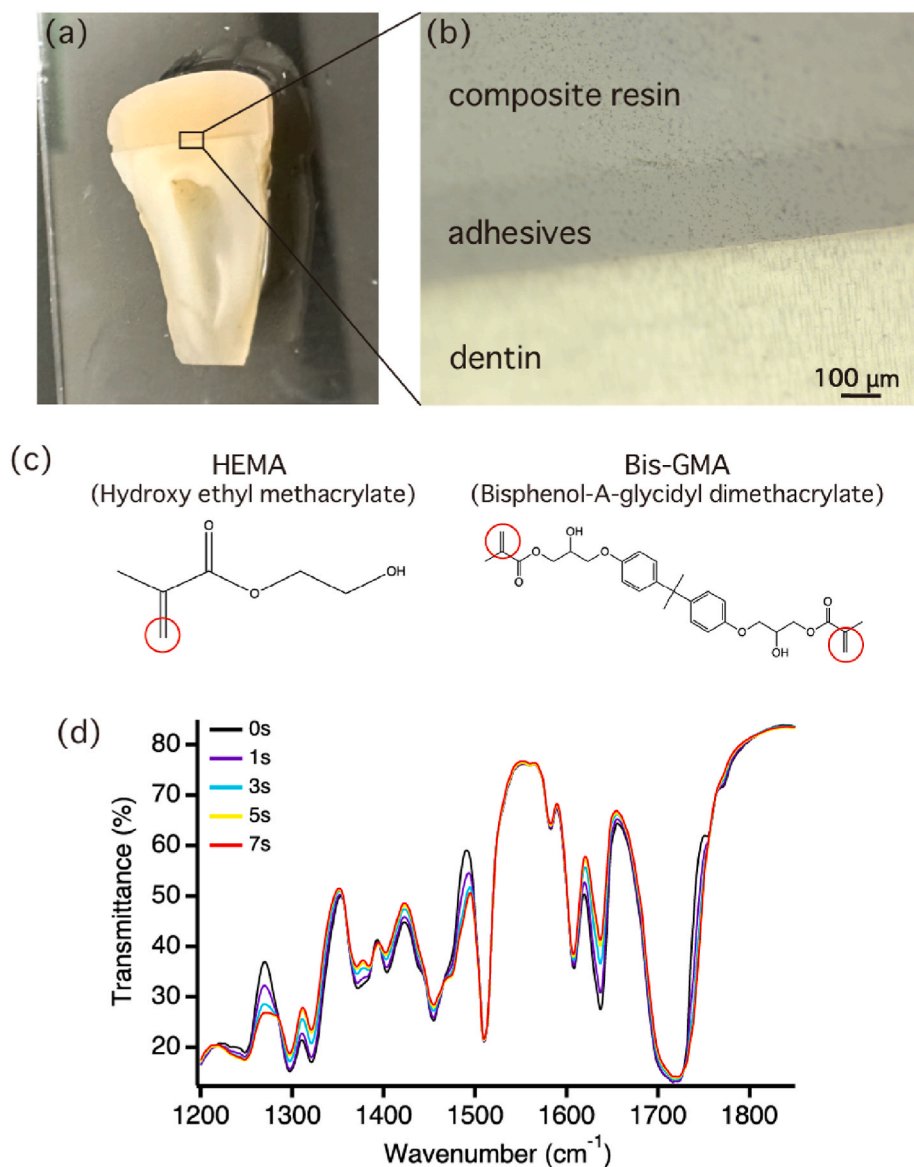


Fig. 1. (a) Photo of human dentin sample. (b) Optical image of human dentin sample at the composite resin/adhesive layers/dentin interface. (c) Chemical structures of dominant monomer components in adhesives. (d) Evolution of IR spectra of adhesive bond upon light illumination.

Fig. S1 in the Supplementary Materials. **Fig. 2(a)**, **(b)**, and **(c)** were constructed using the MIP intensities at 1513 cm^{-1} , 1630 cm^{-1} , and 1080 cm^{-1} , respectively. The upper region represents the adhesive layers and the bottom region represents the dentin. The white dotted lines in the figures indicate the interfaces. In all experiments, both the visible and mid-infrared light were focused on the surface of the sample, and the reflected signal was collected from the solid surface. Given shallow depth of mid-IR light penetration and the large difference in refractive indices between the adhesive (approximately 1.5) and air, the detected signal predominantly originates from the sample surface. In the adhesives, the MIP intensities at 1513 cm^{-1} and 1630 cm^{-1} indicate the predominant contribution of polymerized substances under visible light illumination and monomer constituents, respectively. Notably, the IR signal of aliphatic C=C bonds representing monomer molecules was relatively weak because most of them were polymerized by visible light irradiation. The intensity images of the aromatic and aliphatic C=C bonds exhibited a moderate level of opposing contrast. This implies a local distribution of polymer molecules and uncured monomers. The high signal intensity of the MIP image at 1630 cm^{-1} in dentin originates from the presence of collagens attributed to Amide I bands in the

proteins. Collagens are the primary organic compounds in the dentin. Although the spatial resolution of MIP microscopy was not sufficient to clearly visualize the collagen fibers in the dentin, one can see the fiber structures in the dentin from the MIP image at 1630 cm^{-1} . Furthermore, the contrast of the MIP intensity image at 1080 cm^{-1} was ascribed to the P-O stretching mode, Si-O stretching mode, and C-OH stretching mode, which predominantly represent the distributions of SiO_2 fillers and hydrophilic molecules, both of which are constituents of dental adhesives. The image in the dentin region shows the distribution of hydroxyapatite, which is the predominant component of dentin and consists of calcium phosphate. The variation in the contrast in the adhesive regions for these images indicates the heterogeneous distribution of molecular compositions in dental adhesives at the sub-micrometer scale. Interestingly, the MIP images at 1630 cm^{-1} and 1080 cm^{-1} exhibited a similar contrast, which is in contrast to the MIP image of polymerized molecules at 1513 cm^{-1} . This indicates that the presence of SiO_2 fillers and hydrophilic molecules in dental adhesives may disturb the polymerization of light-cured monomer molecules. **Fig. 2(d)** shows the DC rate of the dental adhesives calculated using the method mentioned above. The image visualizes the micrometer-scale heterogeneity in the DC rate of the

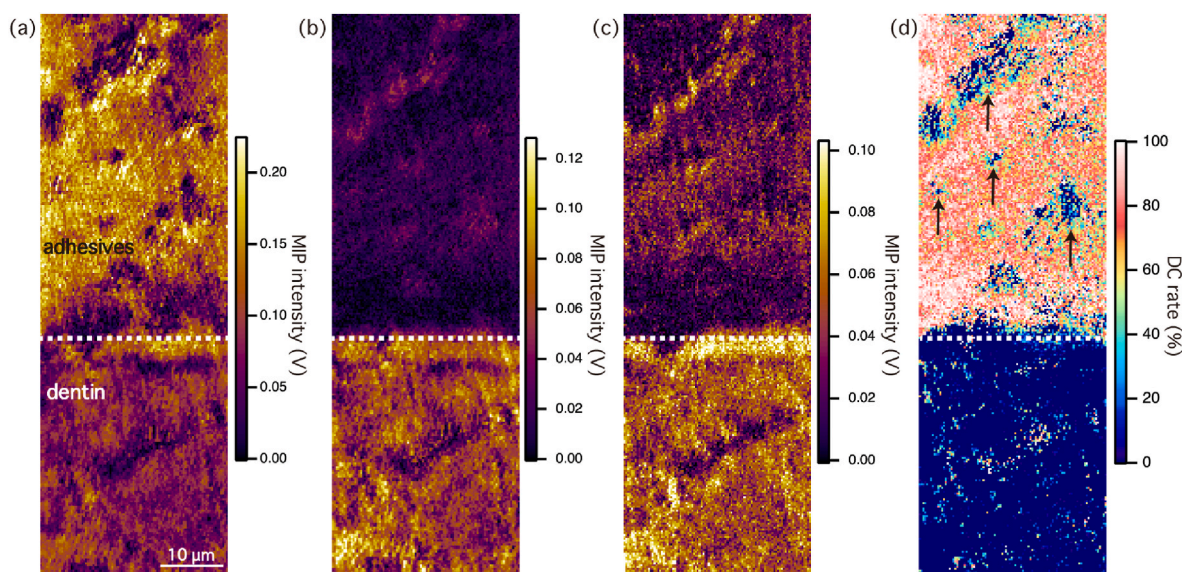


Fig. 2. Hyperspectral mid-infrared photothermal imaging at the interfaces between dentin and dental adhesives. The images were constructed by the MIP intensity at 1513 cm^{-1} (a), 1630 cm^{-1} (b), and 1080 cm^{-1} (c). (d) The DC rate of dental adhesives calculated by the intensity ratio between 1513 cm^{-1} and 1630 cm^{-1} .

clinical dental adhesive samples. The size of the small domains indicated by the black arrows in Fig. 2(d), where uncured monomer molecules are localized, ranges from a few micrometers to tens of micrometers. Conventional FTIR imaging approaches do not allow the observation of such small domains. The DC rate at the interface between dentin and adhesives is crucial for understanding dental adhesive systems. The image shows a low DC rate at the boundary between the dentin and adhesives. It was speculated that the DC rate at the interfaces, particularly near the dentin, would be lower than that at the top surface of the adhesives. We attributed the localized reduction in the DC rate near the dentin to the presence of hybrid layers, in which mineral components are removed and only collagen remains [41]. It is well established that hybrid layers are formed at the interface between dentin and adhesive bonds, typically ranging a few micrometers. These layers consist of collagen and adhesive components. Under such hydrophilic conditions, polymerization of

the adhesive is hindered, resulting in a lower DC rate specifically at the adhesive–dentin interface. The decrease of polymerization degree in the presence of water has been revealed by previous work [42]. The area indicating a low DC rate ranges from a few micrometer-scale scale, which should be somehow reasonable considering the scale of hybrid layers. It is believed that a low DC rate causes bond failure in the oral cavity. The present MIP imaging provides a clear new insight into heterogeneous molecular distribution and the DC rate in dental adhesives of clinical samples, and these findings could not be obtained using conventional analytical approaches.

We further identified regions in which a local decrease in the DC rate occurred with dental adhesives. Fig. 3(a) and (b) show hyperspectral MIP intensity images of the dental adhesives in the vicinity of the dentin at 1513 cm^{-1} and 1630 cm^{-1} , respectively, and Fig. 3(c) depicts the corresponding DC rate for the same area. Fig. 3(d) shows an optical

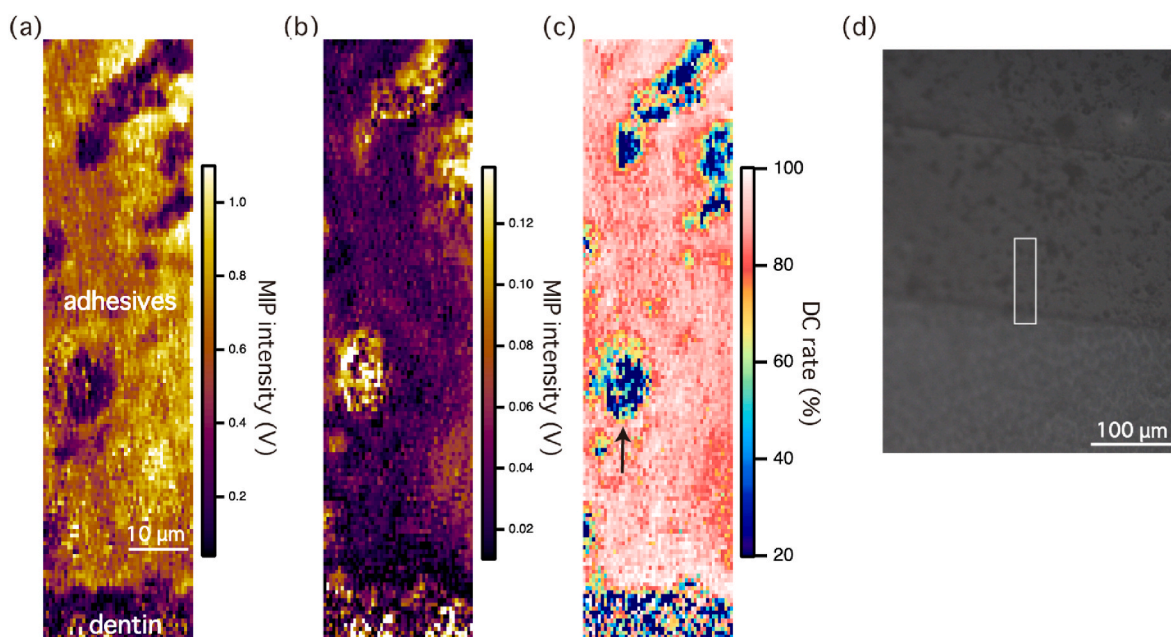


Fig. 3. Hyperspectral mid-infrared photothermal imaging of dental adhesives near the dentin, in which micro-voids are likely present. The images were constructed by the MIP intensity at 1513 cm^{-1} (a), 1630 cm^{-1} (b), and the DC rate (c). (d) An optical microscopy image of the tooth sample.

image of the tooth sample, with a white square indicating the imaging area. Similarly, a moderate degree of opposite contrast was observed between the aromatic and aliphatic C=C bonds in the intensity images, along with a heterogeneous molecular distribution. In the middle region of Fig. 3(c), a localized reduction in the DC rate is evident, forming round structures approximately 5 μm in diameter, as marked by the black arrow. This might be attributed to the presence of micro-voids, such as air bubbles entrapped during the bonding process. It is well known that air bubbles can be formed during the air-blowing and light-curing process of dental adhesives. These air bubbles create what are known as oxygen-inhibited layers, which interfere with the polymerization of the adhesive, leading to the decrease of the DC rate. A previous study suggested that such micro-voids lead to localized weaknesses and compromised bonding durability [19]. Fig. S2 in the Supplementary Materials illustrates an MIP intensity image at 1080 cm^{-1} , where no round structures were observed. This suggests the absence of hydrophilic monomers and SiO_2 fillers in these areas and the presence of uncured monomers following visible light illumination. These results imply that micro-voids hindered the polymerization of monomers in dental adhesives during light-curing process, leading to a localized decrease in the DC rate of adhesive around the bubbles. It should be noted that the “micro-voids” we described in the manuscript correspond to areas where such air bubbles have been present during light curing process, but were absent during measurement. This is why they exhibited strong signals at 1630 cm^{-1} , and low DC rate. The ability of MIP microscopy to resolve IR molecular signatures at the sub-micrometer scale over a large field of view is instrumental in obtaining these insights.

3. Conclusion

In this study, the molecular distribution of clinical tooth samples at the dentin/dental adhesive interface was visualized by MIP microscopy. Hyperspectral sub-micrometer IR imaging revealed heterogeneities in the molecular composition of the adhesives and local variations in the DC rate within the oral cavity. MIP imaging revealed a lower DC rate in adhesives near dentin owing to the presence of hybrid layers. Furthermore, the imaging results suggest that the local decrease in the DC rate in adhesives might be attributed to oxygen-inhibited layers generated during the bonding process. This study highlights the potential application of MIP microscopy in the biochemical analysis of dental materials. The successful visualization of molecular compositions at the sub-micrometer scale was made possible by the autofluorescence-free features of MIP microscopy. Our findings provide valuable insights into the physical and chemical properties of dental adhesives and dentin and contribute to a deeper understanding of the fundamental mechanisms of adhesive bonding. This study paves the way for the development of improved dental treatments and novel adhesive formulations.

4. Experimental section

4.1. Sample preparation

The use of extracted human teeth complied with the ethical review regulations of the Ethics Committee of Tokushima University (329-11). The extracted human maxillary and mandibular molars were immediately stored in refrigerated water at 4 $^{\circ}\text{C}$ and selected for the experiment.

To prepare specimens for observation of the resin-dentin interface, the enamel of the crown was ground to expose a flat dentin surface, which was subsequently polished under running water using #600 waterproof SiC abrasive paper. The exposed dentin was then treated with the self-etching primer of the two-step self-etch system, Clearfil SE Bond 2 (CSE2; Kuraray Noritake Dental, Tokyo, Japan), followed by application of the CSE2 bonding agent. All the bonding procedures were performed according to the manufacturer's instructions. The bonding agent was light-cured for 10 s at 1000 mW/cm^2 in normal mode using an

LED light-curing unit (Pencure 2000, Morita, Tokyo, Japan), equipped with a 15.0 mm tip diameter, following the manufacturer's protocol.

Subsequently, a hybrid resin composite, Clearfil AP-X (Kuraray Noritake Dental, Tokyo, Japan), was incrementally built in 2.0-mm layers. The prepared specimens were stored in water at 37 $^{\circ}\text{C}$ for 24 h and sectioned perpendicular to the tooth root axis using a low-speed saw (ISOMET, BUEHLER, Illinois, USA).

The cross-sectioned surfaces were sequentially polished under running water using #600, #1200, #1500, and #2000 waterproof SiC abrasive papers, followed by mirror polishing with diamond pastes of 6, 3, 1, 0.25 μm , to create the final interfacial observation surface.

4.1.1. Optical setup of MIP microscopy

The configuration of our home-built MIP system is a co-propagating mid-IR and visible beam scheme that enables the MIP observation of bulky opaque samples. A wavenumber-tunable quantum cascade laser (QCL, Daylight Solutions, MIRcat-QT-2100) ranging in wavenumber from 1000 to 1690 cm^{-1} was used as a pulsed mid-IR pump light source for MIP measurements. To avoid photodamage from the mid-IR light, the power of the IR laser after the objective lens was set to less than 0.5 mW for all measurements. The operating repetition rate of the QCL was set to 80 kHz, with a pulse width of 800 ns. A Ge-made long-pass filter reflects approximately 5 % of the IR beam to a mercury cadmium telluride (MCT) detector (Thorlabs, PDAVJ10) to monitor the power spectrum of the QCL for calibration of the MIP spectra. A continuous-wave (CW) visible laser with a wavelength of 561 nm (Cobolt Jive) was used as the probe light source for MIP measurements. The power density of the visible beam was less than 2 mW. The probe beam was passed through a quarter-wave plate and a polarization beam splitter. Both the pump mid-IR and the probe visible beams were co-aligned by a silicon-made dichroic mirror (DM) and subsequently focused on the sample plane with a reflective objective lens (Pike, 40 \times /NA 0.78). The reflected visible probe signal was collected using the same objective and sent to a photodiode (PD, Thorlabs, DET10A2) using a polarization beam splitter. The system had a confocal configuration, where a pinhole with a diameter of 100 μm was set before the photodiode. The current from the PD was sent to the current amplifier (FEMTO, LCA-400K-10 M), the converted voltage was guided to a lock-in amplifier (Zurich Instrument, 500k) for phase-sensitive detection, and the MIP signal was demodulated at the same frequency as the fundamental QCL repetition rate. The spatial resolution of our MIP microscopy in the lateral direction should be defined by the Abbe's diffraction theory. The wavelength of the probe visible laser was 561 nm and the NA of the objective lens for probe light was 0.78. Hence, the theoretical spatial resolution was calculated to be around 440 nm.

For reference measurements, the IR absorption spectra of the samples were measured using a commercially available FTIR spectrometer in the transmission mode (JASCO Corporation, FTIR-6800). The FTIR spectra ranged from 1000 to 3000 cm^{-1} with a spectral resolution of 2 cm^{-1} . For FTIR measurement of adhesives, we fabricated thin adhesive samples, which were sandwiched between two CaF_2 substrates and placed in the FTIR instrument. The sample was irradiated with visible light for curing inside FTIR and subsequently, IR spectra of samples were measured.

CRedit authorship contribution statement

Ryo Kato: Writing – review & editing, Writing – original draft, Visualization, Validation, Methodology, Investigation, Funding acquisition. **Tomiki Iuchi:** Methodology, Investigation. **Yumika Ida:** Methodology. **Kazuhide Yonekura:** Methodology. **Kentaro Takeichi:** Investigation. **Shogo Kawashima:** Writing – review & editing, Methodology, Formal analysis. **Takeo Minamikawa:** Supervision, Data curation. **Takuo Tanaka:** Supervision. **Taka-aki Yano:** Writing – review & editing, Supervision, Funding acquisition, Conceptualization. **Keiichi Hosaka:** Writing – review & editing, Writing – original draft,

Supervision, Conceptualization.

Declaration of competing interest

The authors declare the following financial interests/personal relationships which may be considered as potential competing interests: Ryo Kato reports financial support was provided by Japan Society for the Promotion of Science. Keiichi Hosaka reports financial support was provided by Tokushima University. Keiichi Hosaka reports financial support was provided by Japan Society for the Promotion of Science. Taka-aki Yano reports financial support was provided by Cabinet Office, Government of Japan. If there are other authors, they declare that they have no known competing financial interests or personal relationships that could have appeared to influence the work reported in this paper.

Acknowledgement

This research was supported in part by projects involving Research Cluster Program of Tokushima University (grant nos. 2202006 and 2402003), the Promotion of Regional Industries and Universities by the Cabinet Office, and the Plan for Industry Promotion and Young People's Job Creation by the Creation and Application of Next-Generation Photonics by Tokushima Prefecture. R.K. gratefully acknowledges funding from JSPS KAKENHI (grant no. JP23H04139), Shimadzu Science Foundation, and Research Foundation for Opto-Science and Technology. K.H. acknowledges support from JSPS KAKENHI (grant nos. 20KK0365 and 23K09202).

Appendix A. Supplementary data

Supplementary data to this article can be found online at <https://doi.org/10.1016/j.optcom.2025.132108>.

Data availability

The authors do not have permission to share data.

References

- [1] K. Hosaka, M. Nakajima, M. Takahashi, S. Itoh, M. Ikeda, J. Tagami, D.H. Pashley, Relationship between mechanical properties of one-step self-etch adhesives and water sorption, *Dent. Mater.* 26 (2010) 360–367.
- [2] B. Van Meerbeek, J. De Munck, Y. Yoshida, S. Inoue, M. Vargas, P. Vijay, K. Van Landuyt, P. Lambrechts, G. Vanherle, Buonocore memorial lecture. Adhesion to enamel and dentin: current status and future challenges, *Operat. Dent.* 28 (2003) 215–235.
- [3] S. Nagarkar, N. Theis-Mahon, J. Perdigão, Universal dental adhesives: current status, laboratory testing, and clinical performance, *J. Biomed. Mater. Res. B Appl. Biomater.* 107 (2019) 2121–2131.
- [4] J. Perdigão, Dentin bonding-variables related to the clinical situation and the substrate treatment, *Dent. Mater.* 26 (2010) e24–e37.
- [5] B. Van Meerbeek, K. Yoshihara, Y. Yoshida, A. Mine, J. De Munck, K.L. Van Landuyt, State of the art of self-etch adhesives, *Dent. Mater.* 27 (2011) 17–28.
- [6] F. Ozer, M.B. Blatz, Self-etch and etch-and-rinse adhesive systems in clinical dentistry, *Comp. Cont. Educ. Dent.* 34 (2013) 12–14, 16, 18; quiz 20, 30.
- [7] H. Sano, T. Shono, H. Sonoda, T. Takatsu, B. Ciucchi, R. Carvalho, D.H. Pashley, Relationship between surface area for adhesion and tensile bond strength—evaluation of a micro-tensile bond test, *Dent. Mater.* 10 (1994) 236–240.
- [8] K. Hosaka, J. Tagami, Y. Nishitani, M. Yoshiyama, M. Carrilho, F.R. Tay, K.A. Agee, D.H. Pashley, Effect of wet vs. dry testing on the mechanical properties of hydrophilic self-etching primer polymers, *Eur. J. Oral Sci.* 115 (2007) 239–245.
- [9] M. Peumans, J. De Munck, K.L. Van Landuyt, A. Poitevin, P. Lambrechts, B. Van Meerbeek, A 13-year clinical evaluation of two three-step etch-and-rinse adhesives in non-carious class-V lesions, *Clin. Oral Invest.* 16 (2012) 129–137.
- [10] K. Sato, K. Hosaka, M. Takahashi, M. Ikeda, F. Tian, W. Komada, M. Nakajima, R. Foxton, Y. Nishitani, D.H. Pashley, J. Tagami, Dentin bonding durability of two-step self-etch adhesives with improved degree of conversion of adhesive resins, *J. Adhesive Dent.* 19 (2017) 31–37.
- [11] J. De Munck, K. Van Landuyt, M. Peumans, A. Poitevin, P. Lambrechts, M. Braem, B. Van Meerbeek, A critical review of the durability of adhesion to tooth tissue: methods and results, *J. Dent. Res.* 84 (2005) 118–132.
- [12] I. Nedeljkovic, J. De Munck, A. Vanloy, D. Declerck, P. Lambrechts, M. Peumans, W. Teughels, B. Van Meerbeek, K.L. Van Landuyt, Secondary caries: prevalence, characteristics, and approach, *Clin. Oral Invest.* 24 (2020) 683–691.
- [13] K.L. Van Landuyt, J. Snauwaert, J. De Munck, M. Peumans, Y. Yoshida, A. Poitevin, E. Coutinho, K. Suzuki, P. Lambrechts, B. Van Meerbeek, Systematic review of the chemical composition of contemporary dental adhesives, *Biomaterials* 28 (2007) 3757–3785.
- [14] K. Hosaka, Y. Nishitani, J. Tagami, M. Yoshiyama, W.W. Brackett, K.A. Agee, F. R. Tay, D.H. Pashley, Durability of resin-dentin bonds to water- vs. ethanol-saturated dentin, *J. Dent. Res.* 88 (2009) 146–151.
- [15] E. Asmussen, A. Peutzfeldt, Influence of composition on rate of polymerization contraction of light-curing resin composites, *Acta Odontol. Scand.* 60 (2002) 146–150.
- [16] Q. Ye, J. Park, E. Topp, P. Spencer, Effect of photoinitiators on the in vitro performance of a dentin adhesive exposed to simulated oral environment, *Dent. Mater.* 25 (2009) 452–458.
- [17] Y. Nishitani, M. Yoshiyama, A.M. Donnelly, K.A. Agee, J. Sword, F.R. Tay, D. H. Pashley, Effects of resin hydrophilicity on dentin bond strength, *J. Dent. Res.* 85 (2006) 1016–1021.
- [18] A.M. El Mourad, Assessment of bonding effectiveness of adhesive materials to tooth structure using bond strength test methods: a review of literature, *Open Dent. J.* 12 (2018) 664–678.
- [19] T. Magalhães, R. Fidalgo-Pereira, O. Torres, Ó. Carvalho, F.S. Silva, B. Henriques, M. Özcan, J.C.M. Souza, Microscopic inspection of the adhesive interface of composite onlays after cementation on low loading: an in vitro study, *J. Funct. Biomater.* 14 (2023).
- [20] T. Minamikawa, Y. Harada, N. Koizumi, K. Okihara, K. Kamoi, A. Yanagisawa, T. Takamatsu, Label-free detection of peripheral nerve tissues against adjacent tissues by spontaneous Raman microspectroscopy, *Histochem. Cell Biol.* 139 (2013) 181–193.
- [21] T. Buchwald, Z. Buchwald, Assessment of the Raman spectroscopy effectiveness in determining the early changes in human enamel caused by artificial caries, *Analyst.* 144 (2019) 1409–1419.
- [22] J. Zhang, Y. Liu, H. Li, S. Cao, X. Li, H. Yin, Y. Li, X. Dong, X. Zhang, Discrimination of periodontal pathogens using Raman spectroscopy combined with machine learning algorithms, *J. Innov. Opt. Health Sci.* 15 (2022) 2240001.
- [23] B. Coello, M. López-Álvarez, M. Rodríguez-Domínguez, J. Serra, P. González, Quantitative evaluation of the mineralization level of dental tissues by Raman spectroscopy, *Biomed. Phys. Eng. Express.* 1 (2015) 45204.
- [24] B. Van Meerbeek, H. Mohrbacher, J.P. Celis, J.R. Roos, M. Braem, P. Lambrechts, G. Vanherle, Chemical characterization of the resin-dentin interface by micro-Raman spectroscopy, *J. Dent. Res.* 72 (1993) 1423–1428.
- [25] P. Pongprueksa, J. De Munck, M. Inokoshi, B. Van Meerbeek, Polymerization efficiency affects interfacial fracture toughness of adhesives, *Dent. Mater.* 34 (2018) 684–692.
- [26] R. Kato, T. Umakoshi, P. Verma, Raman spectroscopic nanoimaging of optical fields of metal nanostructures with a chemically modified metallic tip, *J. Phys. Chem. C* 125 (2021) 20397–20404.
- [27] R. Kato, T. Moriyama, T. Umakoshi, T. Yano, P. Verma, Ultrastable tip-enhanced hyperspectral optical nanoimaging for defect analysis of large-sized WS₂ layers, *Sci. Adv.* 8 (2022) eabo4021.
- [28] T. Tanaka, T. Yano, R. Kato, Nanostructure-enhanced infrared spectroscopy, *Nanophotonics* 11 (2022) 2541–2561.
- [29] A. Dazzi, C.B. Prater, AFM-IR: technology and applications in nanoscale infrared spectroscopy and chemical imaging, *Chem. Rev.* 117 (2017) 5146–5173.
- [30] R. Kato, T. Yano, T. Tanaka, Multi-modal vibrational analysis of blend polymers using mid-infrared photothermal and Raman microscopies, *Vib. Spectrosc.* 118 (2022) 103333.
- [31] C. Li, D. Zhang, M.N. Slipchenko, J.X. Cheng, Mid-infrared photothermal imaging of active pharmaceutical ingredients at submicrometer spatial resolution, *Anal. Chem.* 89 (2017) 4863–4867.
- [32] K. Aleshire, I.M. Pavlovic, R. Collette, X.T. Kong, P.D. Rack, S. Zhang, D. J. Masiello, J.P. Camden, G.V. Hartland, M. Kuno, Far-field midinfrared superresolution imaging and spectroscopy of single high aspect ratio gold nanowires, *Proc. Natl. Acad. Sci. U. S. A.* 117 (2020) 2288–2293.
- [33] O. Klementieva, C. Sandt, I. Martinsson, M. Kansiz, G.K. Gouras, F. Borondics, Super-resolution infrared imaging of polymorphic amyloid aggregates directly in neurons, *Adv. Sci.* 7 (2020) 1903004.
- [34] R. Kato, T. Yano, T. Tanaka, Single-cell infrared vibrational analysis by optical trapping mid-infrared photothermal microscopy, *Analyst.* 148 (2023) 1285–1290.
- [35] J. Yin, L. Lan, Y. Zhang, H. Ni, Y. Tan, M. Zhang, Y. Bai, J.X. Cheng, Nanosecond-resolution photothermal dynamic imaging via MHz digitization and match filtering, *Nat. Commun.* 12 (2021) 1–11.
- [36] X. Li, D. Zhang, Y. Bai, W. Wang, J. Liang, J.X. Cheng, Fingerprinting a living cell by Raman integrated mid-infrared photothermal microscopy, *Anal. Chem.* 91 (2019) 10750–10756.
- [37] N.E. Olson, Y. Xiao, Z. Lei, A.P. Ault, Simultaneous optical photothermal infrared (O-ptir) and Raman spectroscopy of submicrometer atmospheric particles, *Anal. Chem.* 92 (2020) 9932–9939.
- [38] N. Baden, H. Kobayashi, N. Urayama, Submicron-resolution polymer orientation mapping by optical photothermal infrared spectroscopy, *Int. J. Polym. Anal. Char.* 25 (2020) 1–7.
- [39] H.J. Haugen, Q. Ma, S. Linskens, M. Par, V.N. Mandic, E. Mensikova, L.P. Nogueira, T.T. Taubock, T. Attin, A. Gubler, S. Leeuwenburgh, M.O. de Bock, D. Marovic, 3D micro-CT and O-PTIR spectroscopy bring new understanding of the influence of filler content in dental resin composites, *Dent. Mater.* 40 (2024) 1881–1894.
- [40] D. Marovic, H.J. Haugen, M. Par, S. Linskens, E. Mensikova, V. Negovetic Mandic, S. Leeuwenburgh, L.P. Nogueira, P.K. Vallittu, Q. Ma, Emerging technologies for

- the evaluation of spatio-temporal polymerisation changes in flowable vs. sculptable dental resin-based composites, *Dent. Mater.* 40 (2024) 1895–1908.
- [41] N. Nakabayashi, M. Nakamura, N. Yasuda, Hybrid layer as a dentin-bonding mechanism, *J. Esthetic Restor. Dent.* 3 (1991) 133–138.
- [42] T. Jacobsen, K.J. Söderholm, Some effects of water on dentin bonding, *Dent. Mater.* 11 (1995) 132–136.